Comparative study of the efficacy of fly ash and reactive aggregate powders in mitigating alkali-silica reaction

Marie Joshua Tapas, PhD (corresponding author)
Research Associate, School of Civil and Environmental Engineering
University of Technology Sydney
Email: mariejoshua.tapas@uts.edu.au

Paul Thomas, PhD
Senior Lecturer, School of Mathematical and Physical Sciences
University of Technology Sydney
Email: Paul.thomas@uts.edu.au

Kirk Vessalas, PhD
Senior Lecturer, School of Civil and Environmental Engineering
University of Technology Sydney
Email: kirk.vessalas@uts.edu.au

Elsie Nsiah-Baafi, PhD
School of Civil and Environmental Engineering
University of Technology Sydney
Email: Elsie.Nsiah-Baafi@uts.edu.au

Liam Martin, PhD student
School of Mathematical and Physical Sciences
University of Technology Sydney
Email: Liam.Martin@student.uts.edu.au

Vute Sirivivatnanon, PhD
Professor, School of Civil and Environmental Engineering
University of Technology Sydney
Email: vute.sirivivatnanon@uts.edu.au

Declarations

Funding
The authors would like to thank ARC Industrial Transformation Research Hub for Nanoscience-based Construction Material Manufacturing (the Nanocomm Hub) and Cement Concrete Aggregates Australia (CCAA) for funding this study.

Conflicts of interest
The authors declare no conflict of interest.

Availability of data and material
The data that support the findings of this study are available from the corresponding author upon reasonable request.

Abstract

This study investigates the ability of reactive aggregate powders to mitigate alkali-silica reaction (ASR) in comparison with fly ash using the accelerated mortar bar test (AMBT). ASR expansion results confirm that the reactive aggregate powders can mitigate ASR, although fly ash still has better mitigating efficacy. Microstructural characterization post-AMBT shows presence of extensive cracking in the plain OPC mortar, few cracks in the mortar with 25% reactive aggregate powders and negligible cracking in the mortar with 25% fly ash. Elemental analysis shows that the reactive aggregate powders are able to increase the Si/Ca and Al/Si ratio of C-S-H composition similar to fly ash. 25% fly ash replacement however results in much higher Si/Ca and Al/Si ratio which likely explains its better efficacy in mitigation. Thermogravimetric analysis results demonstrate that the reactive aggregate powders are pozzolanic like fly ash and that a reactive aggregate powder with better pozzolanic properties has better efficacy to mitigate ASR. The reactive aggregate powders however unlike fly ash do not contribute to compressive strength development of the mortars.

Keywords: alkali-silica reaction; fly ash; reactive aggregate powders; microstructure; ASR gel

Introduction

Alkali-silica reaction (ASR) is a serious durability issue as it may result in premature failure of concrete structures. ASR occurs when the reactive silica component of the aggregate dissolves under the high alkali pore solution of the concrete and reacts with available calcium and alkalis resulting in the formation of alkali-calcium silicate hydrate gel (Na,K-C-S-H) or simply, ASR gel. Susceptible silica phases are those with low crystallinity, many defects in the structure or are amorphous in nature [1].

Supplementary cementitious materials (SCMs) such as fly ash and slag are typically used to mitigate ASR [2]. In Australia, the recommended levels for effective ASR mitigation are 25% fly ash and 50-65% slag [3]. Both fly ash and slag are however industrial by-products and face shortage of supply in the coming years. Fly ash is the waste product from coal-fired power stations whereas slag is from iron manufacturing. Closure of coal-fired power stations in favour of greener energy sources is projected to drastically reduce the supply of fly ash worldwide.

Similarly, slag availability is also only about 5-10% of total cement production and considering slag is being used at higher replacement levels than fly ash, this amount is projected to be insufficient to cover future demands [4].

Since SCMs are highly limited in supply and face shortage in the future, there is a need for alternative SCMs that are both economically viable and sustainable. Several alternative SCMs have been of interest recently [5-11]. Biomass ashes from agricultural wastes like rice husk ash [5, 6], sugarcane bagasse ash [7] as well as ashes from burning of forest wastes and pulp and paper wastes for energy production [12] have shown potential for mitigating ASR. Ground glass is another material of interest due to its impact in reducing glass waste [8-10]. The use of crushed and graded recycled glass fine aggregate in mortar without any deleterious consequences of alkali-silica reaction has been reported, provided sufficient quantity of fine glass powder has been added to the mix [13]. The potential of using ground brick has also been investigated and it has been reported that replacing 25% of cement with ground clay brick (by weight) could significantly decrease the ASR expansion [14, 15].

Recently, there has also been interest in reactive aggregate powders. Since the silica in both SCMs and aggregates react with alkali, the siliceous reactive aggregates have the potential to be used as an alternative SCM. In a study by Cyr et al. [16], it was shown that adding finely ground reactive aggregates led to a reduction in expansion as compared to control mortar. The use of reactive aggregate powders to mitigate ASR supports sustainable construction as there is significant amount of aggregate fines produced during production of manufactured sand as waste. Therefore, other than potential benefits from ASR mitigation, the use of aggregate fines can also reduce waste. However, there is still limited work on the use of reactive aggregate powders on ASR mitigation and the mitigation mechanisms are not well understood.

This study aims to better understand the mitigation mechanisms of reactive aggregate powders and whether these mechanisms are comparable to that of fly ash. Accelerated mortar bar test (AMBT) was carried out by replacing portion of the cement with two reactive aggregate powders (greywacke and dacite) and fly ash. Australian AMBT AS 1141.60.1 which is the most utilized ASR test method in Australia was used to test for the mitigation efficacy of fly ash and reactive aggregate powders [3, 17]. The Australian AMBT is similar to ASTM C1260 except that there is a class of slowly reactive aggregates and a non-reactivity expansion limit of 0.10% at 21 days as specified in Table 4. It also exhibits excellent ability to detect non-reactive aggregates [18]

and in fact a more conservative test method than the concrete prism test (CPT) for determining the required SCM dosage for ASR mitigation [19]. The work of Munir et al. similarly reports on the reliability of AMBT [20].

To investigate the mitigation mechanisms, the calcium silicate hydrate (C-S-H) composition of the mortars was characterized post-AMBT using energy dispersive X-Ray spectroscopy (EDS). Blended pastes with equivalent replacement levels of reactive aggregate powders and fly ash as the mortars were also characterized for portlandite and C-S-H content after exposure to AMBT conditions. Compressive strength test of mortars with and without reactive aggregate powders cured under normal hydration and AMBT conditions was also carried out to determine the effect of the reactive aggregate powders on hardened properties.

2.0 Materials and Methods

2.1 Raw Materials

A general purpose cement (type GP) with 7.5% mineral addition, conforming to Australian Standard AS 3972 *General Purpose and Blended Cement* [21] was used in this study. The fly ash used complies with AS 3582.1 *Supplementary Cementitious Materials for Use with Portland and Blended Cement Part 1: Fly ash* [22]. Reactive aggregates greywacke and dacite manufactured sands (graded in accordance with AS 1141.60.1) and Waikato natural sand were used. To obtain reactive aggregate powders used as an alternate SCM, the aggregates were finely ground using a ring mill for five minutes.

Table 1 lists the oxide compositions of cement, SCMs, and the reactive aggregates utilized in the study. XRF analysis was carried out at the Mark Wainwright Analytical Centre, University New South Wales (UNSW) using a PanAnalytical PW2400 XRF Rh end-window tube coupled with "SUPERQ" software. A non-reactive sand (Normensand, EN 196-1) was also used for compressive strength test. Table 2 shows the particle size distribution (PSD) of the raw materials measured by laser diffraction using Malvern MasterSizer 2000 using either isopropanol (for samples that were prone to hydration) or water as the dispersion medium. The powders were dispersed in appropriate solvent in beakers using an ultrasonic bath.

Table 1 XRF Analysis of the cement, SCMs and aggregates

Oxide wt%	GP Cement	Fly Ash	Greywacke	Dacite	Waikato
SiO_2	19.67	59.21	66.85	68.4	62.93
TiO_2	0.22	1.11	0.65	0.4	0.55
Al_2O_3	4.78	28.11	14.24	13.3	14.21
Fe_2O_3	3.1	3.68	3.8	3.3	4.45
Mn_3O_4	0.12	0.11	0.09	0.1	0.09
MgO	0.91	0.53	1.58	1.3	1.43
CaO	64.18	2.48	1.94	2.4	3.46
Na_2O	0.33	0.63	4.25	2.4	4.31
K_2O	0.41	1.18	3.11	3.8	1.09
P_2O_5	0.06	0.41	0.14	0.1	0.04
SO_3	2.37	0.16	0.19	<0.01	<0.01
L.O.I.	4.09	1.05	2.29	4.1	7.08

Table 2 PSD analysis of the raw materials

Raw Material	D (0.1) µm	D (0.5) µm	D (0.9) µm
Cement	3.74	16.11	39.28
Fly Ash	0.97	17.12	63.23
Greywacke powder	2.44	30.50	99.21
Dacite powder	2.14	41.19	96.22

2.2 Accelerated Mortar Bar Test

Accelerated mortar bar test (AMBT) was carried out to evaluate the effect of substituting portion of the cement with reactive aggregate powders on ASR mitigation. Mortar bars composed of 1 part of cement to 2.25 parts of graded aggregate by mass (440 g cement per 990 g of aggregate) and water to cementitious materials ratio equal to 0.47 by mass were prepared in accordance to AS 1141.60.1 [17]. The reactive aggregate powders were used at a cement replacement level of 25% by mass. Mortar with 25% fly ash cement replacement level (by mass of cement) was also prepared for comparison.

The specimens were prepared in 25 x 25 x 285 mm moulds with a gauge length of 250 mm then cured in high humidity environment at room temperature (23±2 °C) for 24 hours. After, the specimens were carefully de-moulded and put in a container filled with water. The container was then placed in an oven set at 80 °C for 24 hours to allow the specimens to slowly equilibrate to 80 °C. After which, zero-hour length measurements were obtained using a horizontal comparator prior immersing the specimens in 1M NaOH solution at 80 °C for

28 days. Succeeding expansion measurements were obtained at 1, 3, 7, 10, 14, 21, and 28 days. Three readings were taken per mortar specimen at each age. Total expansion incurred by the aggregate after 10 days and 21 days of NaOH immersion was used to classify its ASR potential in accordance with AS 1141.60.1. Since Australia does not have an existing standard for assessing the efficacy of SCMs in ASR mitigation, the same criteria were employed for mixes with SCMs as it is very similar to widely recognized ASTM C1567 [23]. The classification criteria are shown in Table 4.

Table 3 Aggregate grading requirements

Sieve size, mm		% mass
Passing	**Retained on**	
4.75	2.36	10
2.36	1.18	25
1.18	0.60	25
0.60	0.30	25
0.30	0.15	15

Table 4 AMBT expansion criteria (AS 1141.60.1)

Mean mortar bar expansion %		
Duration of specimens in 1M NaOH 80 °C		
10 days	**21 days**	**Reactivity classification**
---	E<0.10*	Non-reactive
E<0.10*	0.10*≤E<0.30	Slowly reactive
E≥0.10*	---	Reactive
---	0.30≤E	Reactive

*For naturally occurring fine aggregates the limit is 0.15%

2.3 Microstructural Characterization of Mortars Post-AMBT

Microstructural analysis was carried out on the mortars post-AMBT. The mortars were cut with diamond saw and then immersed in isopropanol for seven days to remove free water (solvent exchange method). After which, epoxy resin was used to mould the cut mortar and once hardened (24 hours curing), polishing was carried out using Struers automated polishing machine. MD Largo disc and various sizes of diamond sprays (9µm, 3µm and 1µm) were used to ensure optimal polishing quality. The polished sections were allowed to dry in a vacuum desiccator for two days prior being subjected to imaging and elemental analysis.

Scanning electron microscopy and energy dispersive X-ray spectroscopy (SEM-EDS) was carried out using FEI Quanta 200 with Bruker XFlash 4030 EDS detector. SEM was operated in backscattered electron (BSE) mode, 15 kV accelerating voltage and 12.5mm working distance. The composition of C-S-H was measured by point EDS analysis on the hydration rims around the hydrated clinker (inner C-S-H) following the method of Rossen and Scrivener [24].

2.4 Pozzolanic Behaviour and Phase Evolution under AMBT conditions

In order to characterize the pozzolanicity of the aggregates, paste specimens with 25% replacement levels of reactive aggregate powders were prepared using electronic mixer and cured for one day in a temperature and humidity cabinet set at 90%RH 23±2 °C. After one day curing, the paste specimens were transferred to an AMBT bath (1M NaOH 80 °C). Conditions comparable to AMBT were employed to mimic the environment present during accelerated testing. Plain cement paste (OPC) was also prepared to serve as a reference. Thermogravimetric (TG) and X-ray diffraction (XRD) data were obtained at 7 and 21 days.

TG curves in this study were obtained using TA Instruments SDT-Q600 Simultaneous TGA/DSC equipment. The paste specimens were ground using mortar and pestle and 50 mg sample was taken from the ground material, and transferred to a platinum crucible, which was then placed inside the TG instrument. The thermal analysis was performed in a nitrogen gas atmosphere, within a temperature range from 23 °C to 1000 °C and at a heating rate of 10 °C/min. To supplement the TG studies and get an indication of the reactive silica content of the fly ash and the reactive aggregate powders, a dissolution test was also carried out. For the dissolution test, 5 grams of the powder (fly ash or reactive aggregate powders) was immersed in 50ml sealed 1M NaOH 80 °C and 2ml aliquots were obtained at 7, 14 and 21 days. These were then diluted (10x, 100x and 1000x), acidified with high purity nitric acid and then subjected to ICP-OES (inductively coupled plasma - optical emission spectrometry) for analysis of dissolved silicon. The results reported in this paper have taken into account the dilution factor.

For XRD analysis, the blended pastes were powdered using mortar and pestle and then carefully loaded into the XRD sample holders (front loading), ensuring to not over press the surface to prevent the preferred orientation.

XRD patterns were obtained using a Bruker D8 Discover XRD in Bragg-Brentano mode using Cu Kα radiation (1.5418 Å) from 5° to 80° 2θ at a scan rate of 0.04°/s. Phases were identified using the ICDD PDF 4+ database.

2.6 Effect of reactive aggregate powders on compressive strength development

In order to investigate the effect of replacing cement with reactive aggregate powders on compressive strength, mortar prisms with dimension 40mm x 40mm x 160mm were prepared and tested in accordance with AS 2350.11 (loading rate is 2.4kN/ sec) using a Universal Testing Machine (Shimadzu UH-500kN XR). Compressive strength test was carried out on the two ends of each prism (on the side faces) over an area of 40 mm x 40 mm and the compressive strength is reported as an average of two breaks. A jig was used during the compression test to ensure consistency in the measured strength results (see Figure 1).

Two types of sand were used for the mortar, a non-reactive sand (NR Sand) and reactive sand Waikato. The use of non-reactive sand is to eliminate the influence of ASR expansion arising from the fine aggregate that may influence compressive strength results. The binder was replaced with either 25% reactive aggregate powders or fly ash and the sand was dried in the oven for 24 hours before casting to ensure consistent w/binder ratio. To achieve a workable mix, 0.45w/c ratio was used for the non-reactive sand, whereas 0.60 w/c was used for the finer sand Waikato. The non-reactive sand and Waikato are both natural sands (i.e. river sand).

One set of the mortars was stored at AMBT conditions (1M NaOH 80 °C) and another in a thermal cabinet at 90%RH 23 °C. The mix designs for the mortars are listed in Table 5.

Table 5 Mortar mixes subjected to compression test

*Sand/ Fine aggregate	Curing Conditions	Mass (grams)				
		OPC	Fly ash	Dacite Powder	Greywacke Powder	Sand/Fine Aggregate
NR Sand	90RH 23 °C	450.0	0.0	0.0	0.0	1350.0
NR Sand	90RH 23 °C	337.5	112.5	0.0	0.0	1350.0
NR Sand	90RH 23 °C	337.5	0.0	112.5	0.0	1350.0
NR Sand	90RH 23 °C	337.5	0.0	0.0	112.5	1350.0
NR Sand	80 °C 1M NaOH	450.0	0.0	0.0	0.0	1350.0
NR Sand	80 °C 1M NaOH	337.5	112.5	0.0	0.0	1350.0
NR Sand	80 °C 1M NaOH	337.5	0.0	112.5	0.0	1350.0
NR Sand	80 °C 1M NaOH	337.5	0.0	0.0	112.5	1350.0
Waikato	80 °C 1M NaOH	450.0	0.0	0.0	0.0	1350.0
Waikato	80 °C 1M NaOH	337.5	112.5	0.0	0.0	1350.0
Waikato	80 °C 1M NaOH	337.5	0.0	112.5	0.0	1350.0
Waikato	80 °C 1M NaOH	337.5	0.0	0.0	112.5	1350.0

*The sand/fine aggregate was tested and classified as per AS 1141.60.1

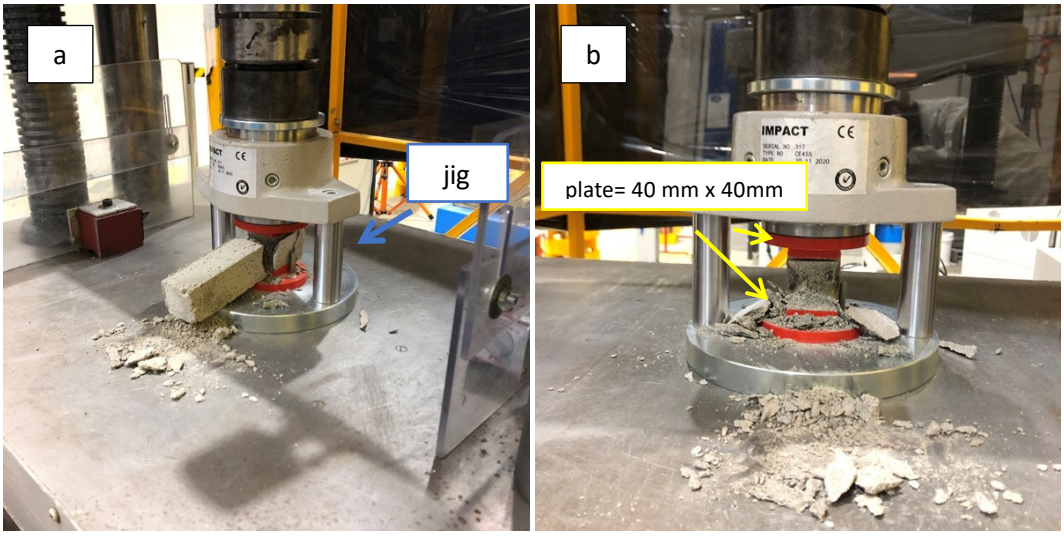

Figure 1 Compression test set-up based on AS 2350.11 (loading rate is 2.4kN/ sec) showing the jig placed in between the platens of the machine to transmit the load of the machine to the compression surfaces of the mortar specimens, a) side view and b) front view

3.0 Results and Discussions

3.1 AMBT Expansion Results

Figures 2 and 3 show the efficacy of various reactive powders to mitigate ASR expansion using two types of reactive aggregate (manufactured sand greywacke and river sand Waikato). Figure 2 shows the measured

expansion of the greywacke mortar with two types of reactive aggregate powders (greywacke, dacite) and fly ash. Greywacke powder is notably better than dacite in reducing ASR expansion showing ability to reduce expansion to less than 0.10% at 21 days making the system unreactive as per criteria outlined in Table 4. Greywacke powder mitigating greywacke is also in effect self-mitigation. This indicates that a reactive aggregate finely ground will have an opposite effect on ASR than if used as a regular aggregate. Dacite also significantly reduces expansion, although lower efficacy than greywacke. Dacite powder is able to reduce expansion to lower than 0.10% at 10 days, but expansion exceeds 0.10% at 21 days making the system slowly reactive as per AS 1141.60.1. Figure 3 shows the ability of reactive aggregate powder greywacke to mitigate ASR when used in conjunction with a reactive natural sand (Waikato river sand). The expansion limit was adjusted to 0.15% based on AS 1141.60.1 specification for natural sand. Greywacke powder again was able to successfully mitigate ASR (i.e. the expansion was reduced to below 0.15% at 10 and 21 days). It is however worth noting that 25% fly ash is still the best for ASR mitigation as shown in Figures 2 and 3. The better efficacy of fly ash may be related to its higher amorphous silica and alumina content as well as finer PSD [2].

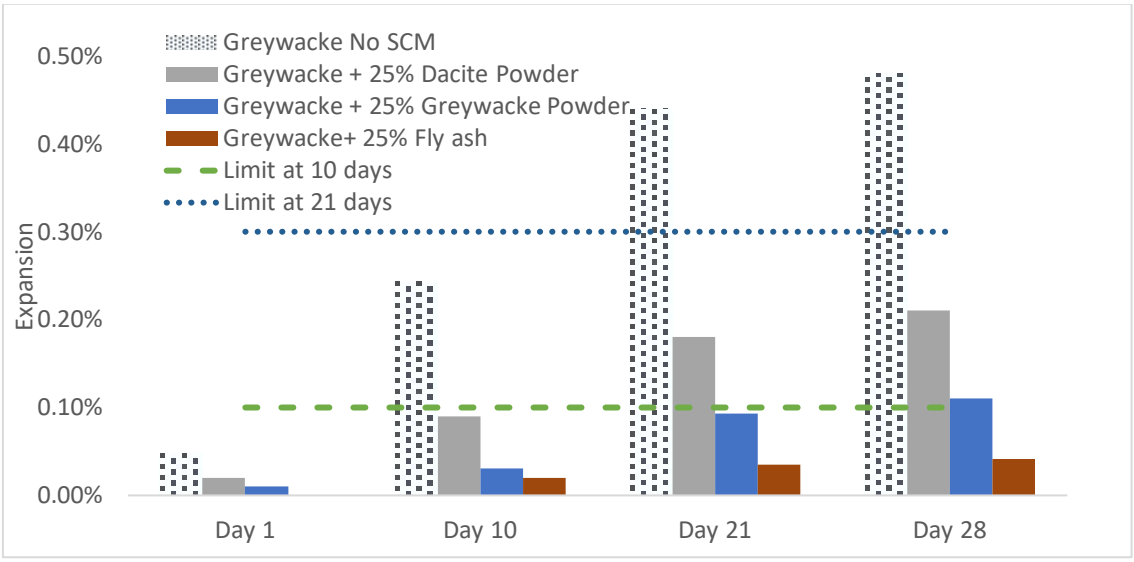

Figure 2 AMBT expansion of greywacke mortar with various reactive aggregate powders at 25% replacement level (dacite and greywacke) and fly ash

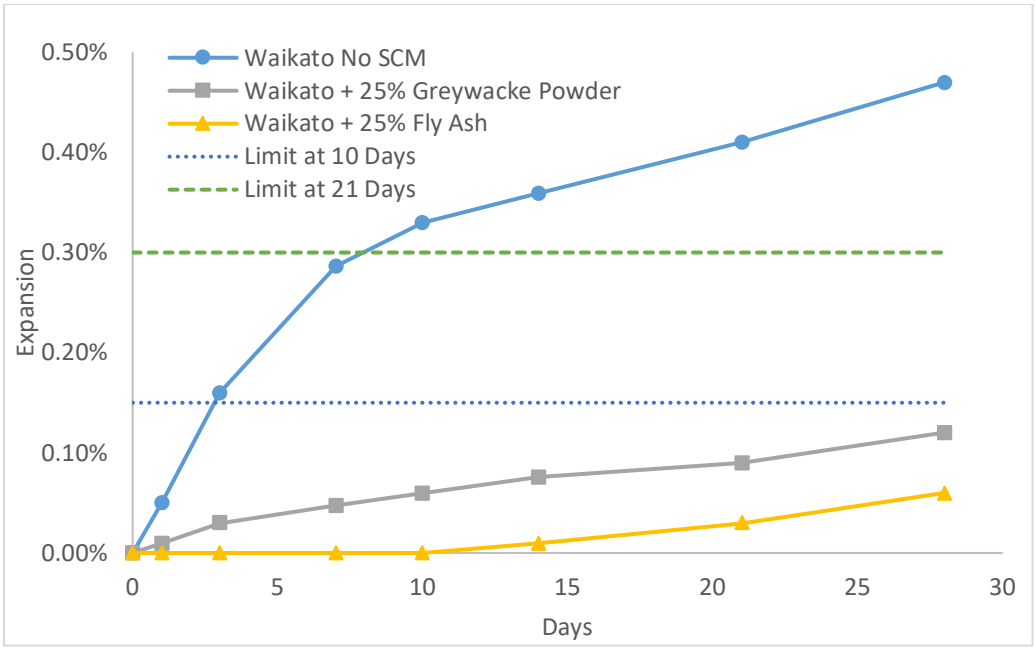

Figure 3 AMBT expansion of reactive river sand (Waikato natural sand) with and without 25% replacement of reactive greywacke powder and 25% fly ash

3.2 Characterization of the Mortars Post-AMBT and ASR Gel Composition

The greywacke mortars with no SCM (OPC only), 25%GW powder and 25%DC powder subjected to AMBT were sectioned and low magnification SEM images are shown in Figure 4. The greywacke mortar without SCM (Figure 4a) shows extensive cracking. The presence of cracks is also notable even in mortars with reactive aggregate powders, albeit less. This is consistent with the slight expansion observed in Figure 2. The mortar with 25% fly ash on the other hand hardly shows any cracking. The higher porosity of the OPC mortar is also notable in Figure 4. The mortar with 25% fly ash exhibits the most dense microstructure.

Figure 5 shows the EDS X-ray map of the ASR gel found in the mortar with 25% greywacke powder. This area corresponds to the region boxed in red in Figure 4b. The ASR gel is dominated by sodium (Na), silicon (Si) and calcium (Ca). The negligible amount of potassium (K) detected indicates that the pore solution is dominated by Na due to the 1M NaOH storage solution consistent with what has been reported in other AMBT studies [25, 26]. ASR gel in concrete prisms and field studies contains considerable amount of potassium [26, 27]. The high

concentration of calcium (Ca) observed is consistent with the ASR gel being alkali-calcium-silicate hydrate [27, 28]. The red (Si) and yellow (Al) areas surrounding the crack confirms the composition of silica and alumina-rich greywacke aggregate. Table 6 lists the EDS point analysis results of the ASR gel. The points analysed are shown in Figure 5a. The ASR product has an average Ca/Si ratio of 0.24 and (Na+K)/Si of 0.34 consistent with that reported in literature [26-30].

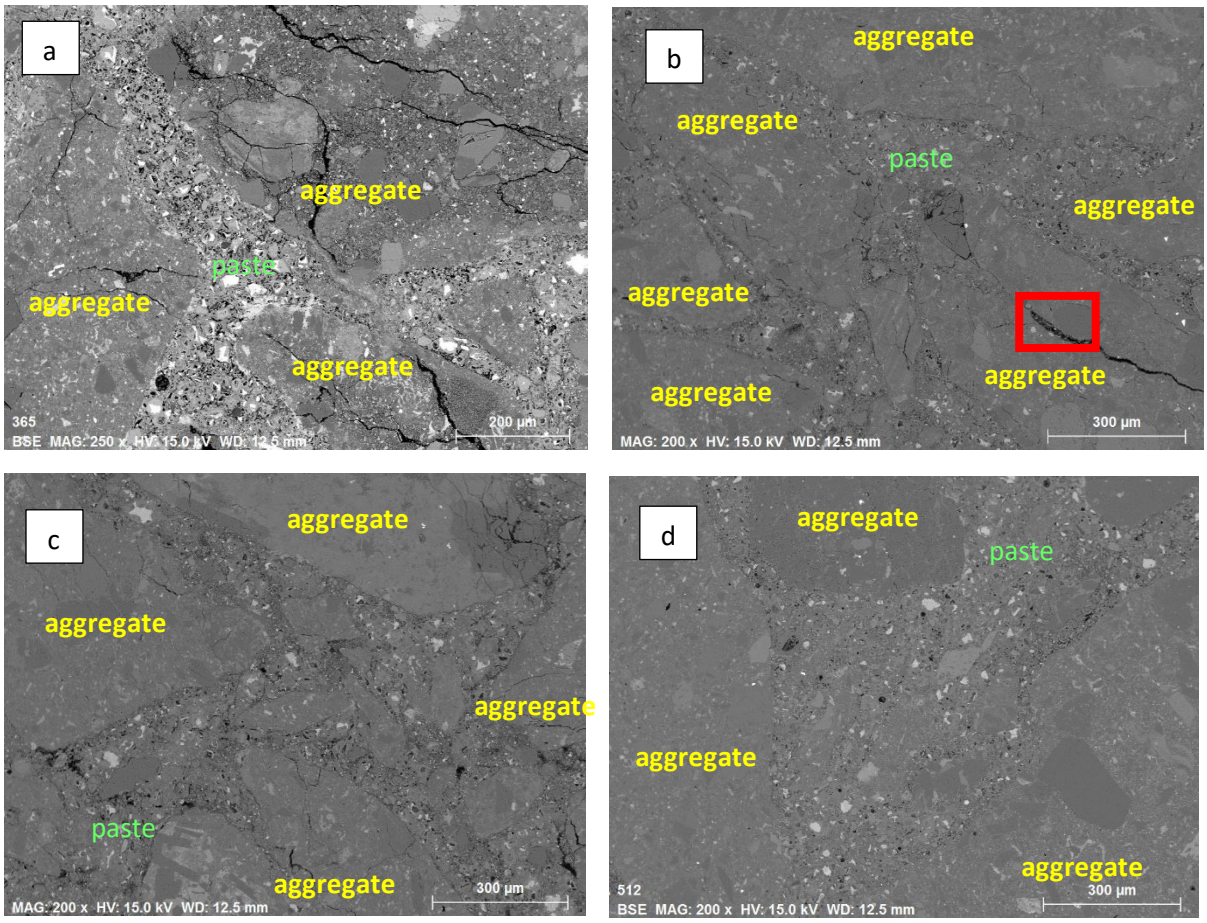

Figure 4 SEM images of a) GW mortar with no SCM, b) GW mortar+25%GW, c) GW mortar +25%DC and d) GW mortar+25%FA

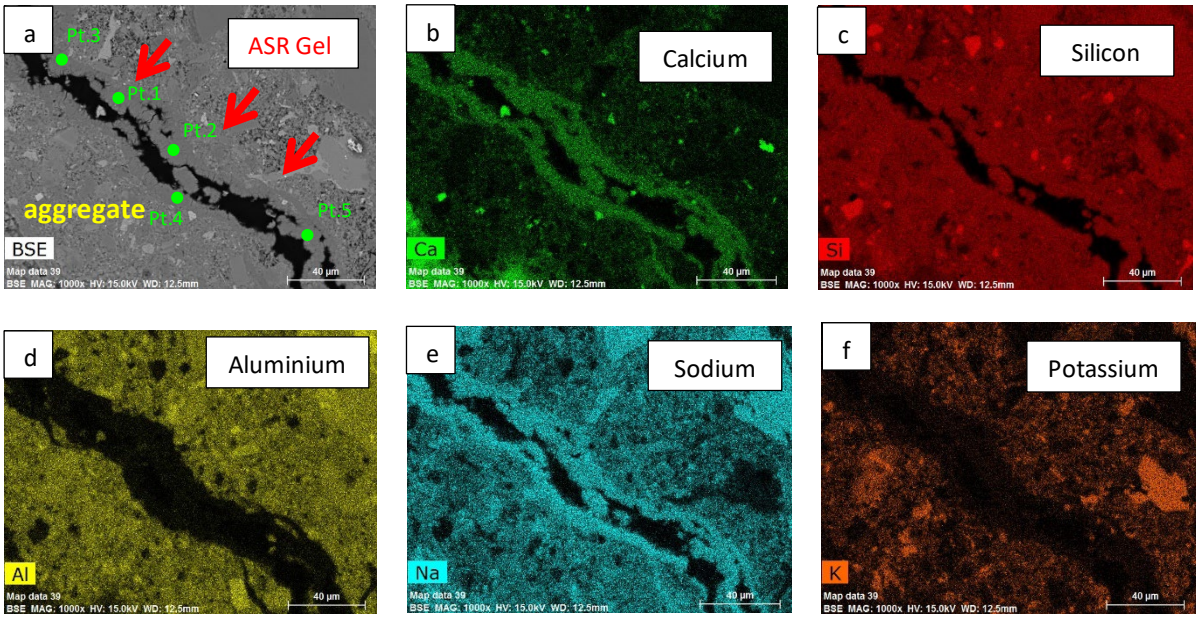

Figure 5 EDS X-ray map of sectioned GW mortar+25% greywacke powder (a) showing the concentration of the elements in the ASR product: calcium (b), silicon (c), aluminium (d), sodium (e) and potassium (f)

Table 6 Elemental analysis of the ASR gel in mortar +25% GW powder

EDS Location	atomic weight%								
	Ca	Al	Si	O	Na	K	Na+K	Ca/Si	(Na+K)/Si
ASR Gel Pt 1	5.92	0.91	24.29	60.45	7.62	0.26	7.88	0.24	0.32
ASR Gel Pt 2	7.49	0.57	23.61	59.94	7.87	0.34	8.21	0.32	0.35
ASR Gel Pt 3	5.69	0.79	24.35	60.40	8.17	0.13	8.30	0.23	0.34
ASR Gel Pt 4	5.13	0.95	24.22	60.22	8.53	0.15	8.68	0.21	0.36
ASR Gel Pt 5	4.71	0.79	24.83	60.63	8.27	0.09	8.36	0.19	0.34
Average	5.79	0.80	24.26	60.33	8.09	0.19	8.29	0.24	0.34
STDEV	1.06	0.15	0.43	0.26	0.35	0.11	0.29	0.05	0.01

Figure 6-8 shows the EDS X-ray map of the paste portion of the mortars showing distribution of phases. Sodium (Na) is dominant in the paste regions consistent with immersion in a 1M NaOH storage solution. Negligible potassium (K) is observed in the pastes. Figures 6 and 7 still show presence of unreacted reactive aggregate powders while Figure 8 shows presence of unreacted fly ash. The reactive aggregate powders and fly ash are both identified by the Si (red) or both Si and Al-rich (yellow) regions. Portlandite (areas with high calcium concentration, i.e. prominent green regions), mostly adjacent to the aggregate powders, was also found uniformly distributed in the paste. The mortar with 25% fly ash shows less portlandite than the mortars with reactive aggregate powder suggesting higher pozzolanicity of fly ash.

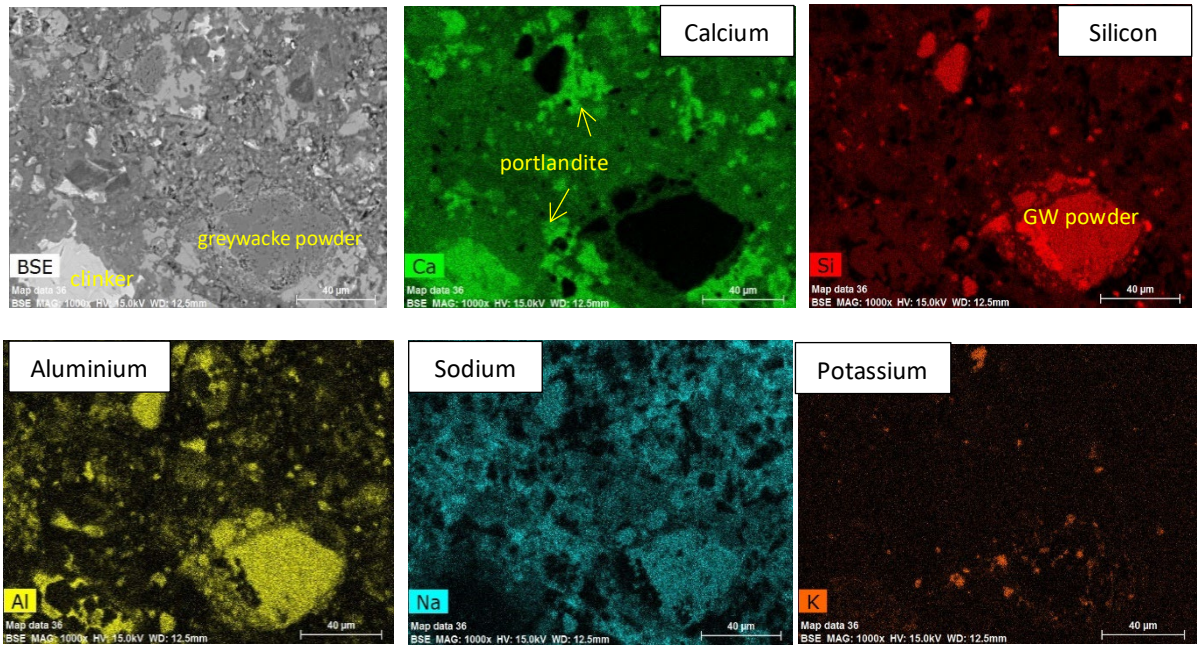

Figure 6 EDS X-Ray map of the GW mortar with 25% greywacke powder

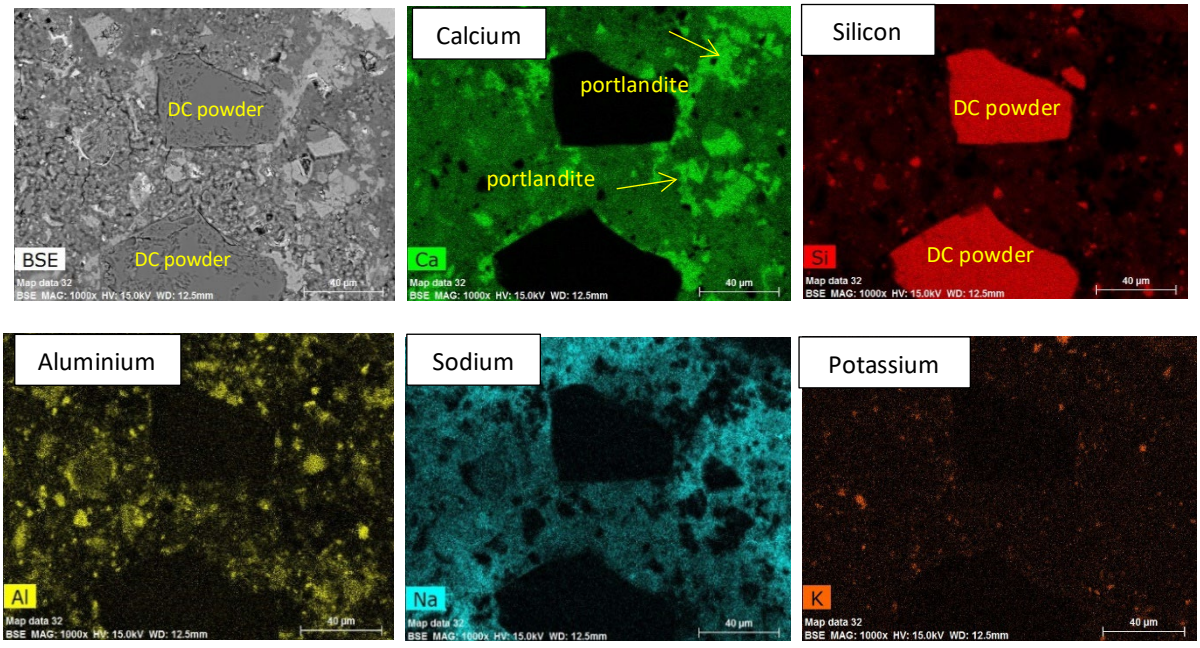

Figure 7 EDS X-Ray map of GW mortar with 25% dacite powder

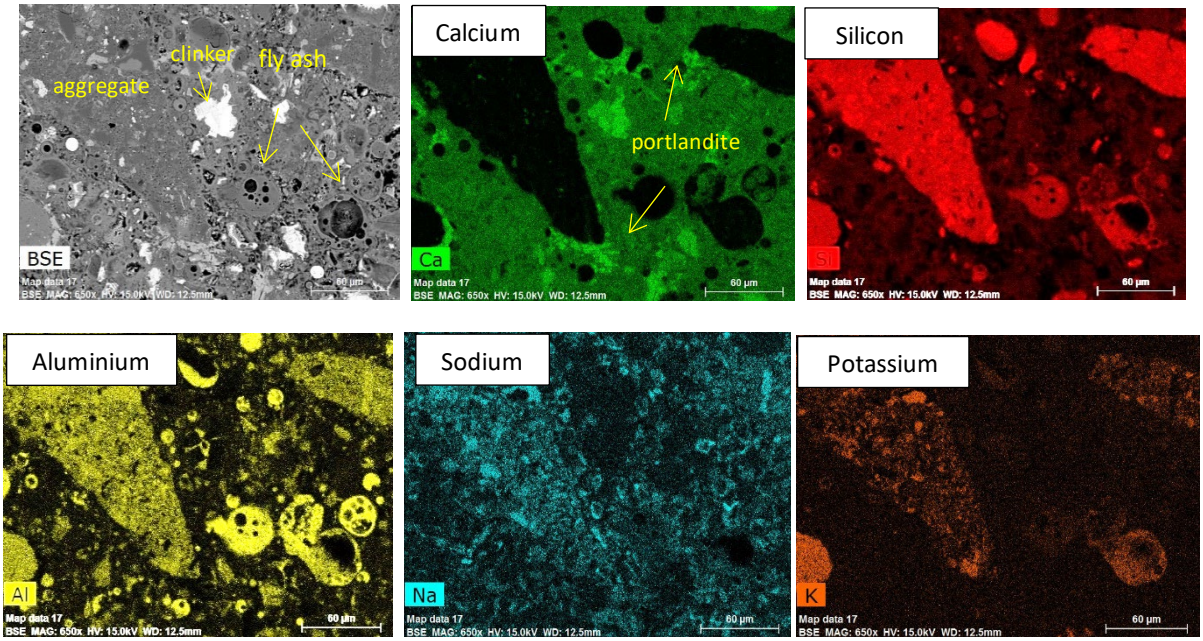

Figure 8 EDS X-Ray map of the GW mortar with 25% fly ash powder

Figure 9 shows the EDS scatter plot of the Si/Ca vs Al/Si ratio of the C-S-H of the greywacke mortars. The Si/Ca ratio of mortars with reactive aggregate powders were found to be higher than that of mortar with cement only and almost comparable to the mortar with 25% fly ash. The higher the Si/Ca ratio, the higher the alkali binding capacity of the C-S-H [2]. GW mortar+25%FA however has notably higher Al/Si ratio than the mortars with reactive aggregate powders. Amongst two reactive aggregate powders, greywacke powder has higher Al/Si ratio. This likely explains the better efficacy of fly ash and greywacke powder at similar dosage to mitigate ASR expansion than dacite powder. A study by Hong and Glasser reported that the aluminium can be further incorporated into the pozzolanic reactions to form C-A-S-H (also known as Al-modified C-S-H) gel which has enhanced alkali binding capacity [31, 32]. The incorporated aluminium in the Si-O-Si layers leads to a free negative valence, resulting in the compensation of this charge by the positive alkali ions Na^+ and K^+.

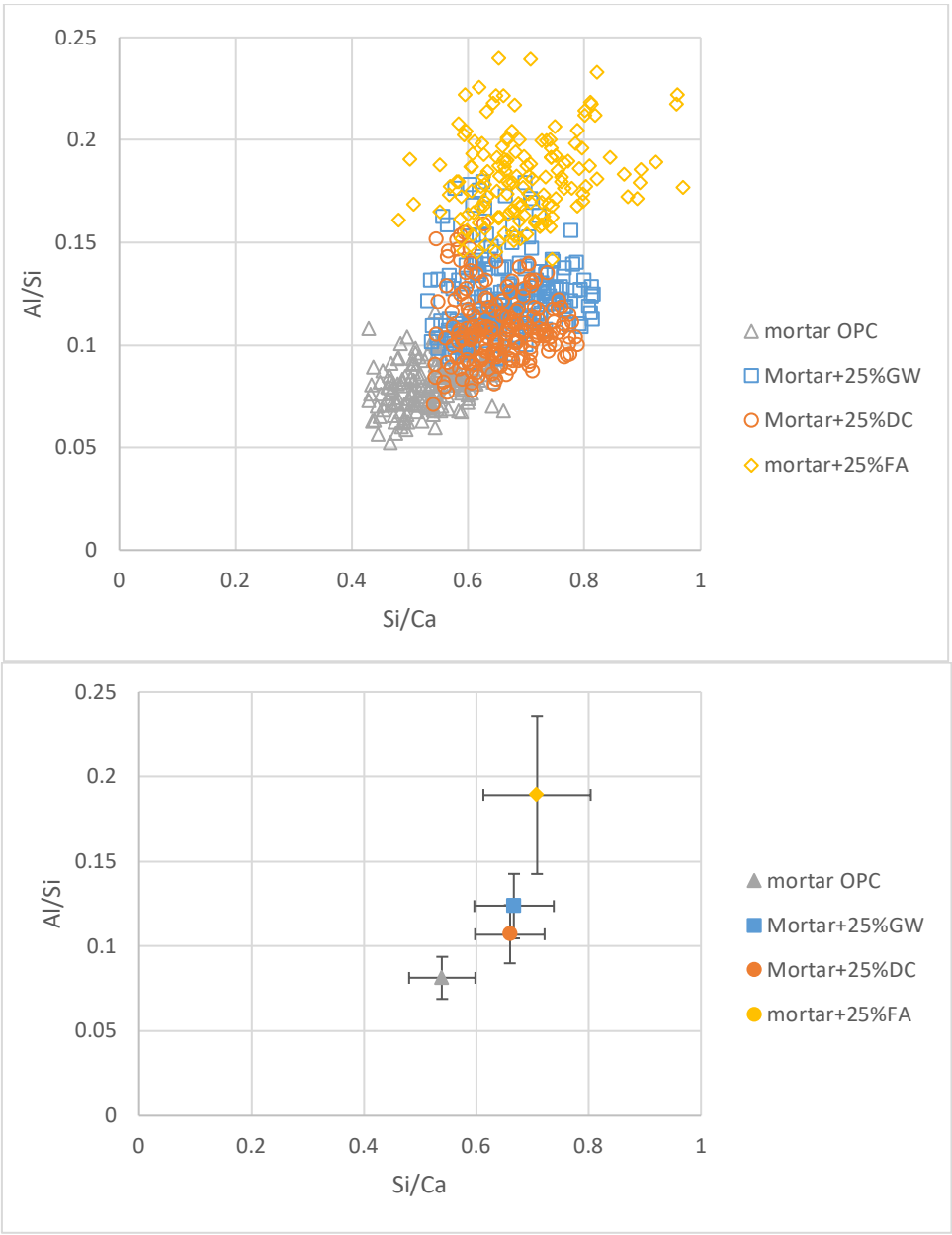

Figure 9 EDS analysis of the greywacke mortars showing the Al/Si and Si/Ca ratios of the C-S-H reported as a) scatter plot of ~200 points per sample and b) average of the points showing the STDEV

3.3 Pozzolanic Behaviour of the Reactive Aggregate Powders and Fly ash

Figure 10 shows the DTG results for OPC and OPC with 25% replacement of fly ash and reactive aggregate powders (paste samples) after 7 days exposure to AMBT conditions. There are three main peaks notable in the DTG curve: the decomposition of C-S-H ≤200 °C, the dehydroxylation of calcium hydroxide (CH), [$Ca(OH)_2$ → CaO + H_2O] at about 400-500 °C, and the decarbonation of calcium carbonate, $CaCO_3$ [$CaCO_3$ → CaO + CO_2] which

367 occurs between 600 °C and 800 °C [33]. The absence of carboaluminate and ettringite peaks/shoulders at about
368 100 to 200 °C is because of their instability under AMBT conditions as confirmed from the XRD results in Figure 13
369 and consistent with what has been reported in another study [26]. Other studies have also reported that both
370 ettringite and carboaluminate are only stable up to 70 °C and starts to decompose at higher temperatures [34,
371 35]. In the DTG plot, the smaller the area of the curve, the lower the amount of hydrate present/remaining in
372 the binder system. Comparing the area under the curve at about 400-500 °C (CH region), it can be observed that
373 the pure cement binder has the highest amount of CH remaining and all pastes with 25% reactive aggregate
374 powder or fly ash replacement showed much lower amount of portlandite than reference OPC. OPC+25%FA has
375 the least amount of portlandite remaining (i.e. higher CH consumption) followed by OPC+25%GW and
376 OPC+25%DC. The higher the portlandite consumption, the more pozzolanic is the material. Results therefore
377 demonstrate that like fly ash, the reactive aggregate powders are pozzolanic materials. The ability of fly ash and
378 the reactive aggregate powders to consume portlandite follows a similar trend as their ability to reduce
379 expansion. The pozzolanic behaviour of the aggregate fines correlates with their efficacy as SCMs for ASR
380 mitigation and the higher the degree of pozzolanicity, the higher the efficacy in ASR mitigation [2].
381
382 From Figure 10, it is also worth noting that cement has the least amount of C-S-H produced at 7 days while
383 OPC+25%FA has the most C-S-H produced. Both binder systems with reactive aggregate powders also
384 demonstrate higher amount of C-S-H formed than pure cement. Similarly, it is notable that the amount of C-S-H
385 produced is proportional to the ability of the binder to mitigate ASR: OPC+25%FA> OPC+25%GW>OPC+25%DC.
386 Aside from producing C-S-H, the consumption of CH indicates reduced amount of calcium available for the
387 formation of expansive ASR gel [36].
388

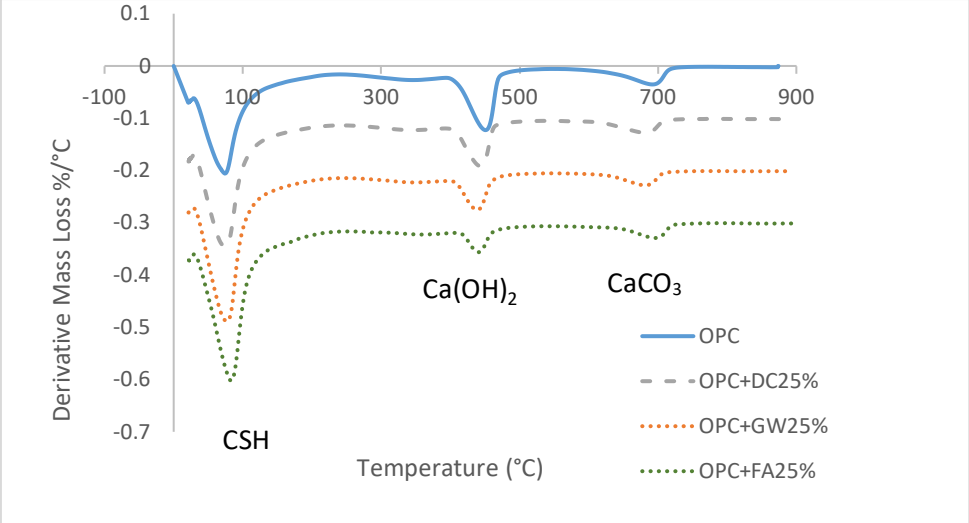

Figure 10 DTG curves showing portlandite remaining in the pastes after 7 days immersion in 1M NaOH 80 °C

The ability of the reactive aggregate powders to mitigate ASR is beyond cement dilution effect as demonstrated by the effect of the type of aggregate powder on the ability to reduce expansion. This indicates that the composition of the aggregates, in particular the amorphous content, affects the pozzolanic behaviour and consequently, the ASR mitigation efficacy. The pozzolanic activity is indicated by the available silica or "amorphous silica" content which reacts with portlandite to form secondary C-S-H. To get an indication of the reactive silica content, fly ash and the reactive aggregate powders were immersed in 1M NaOH 80 °C and 2ml aliquots were obtained at 7, 14 and 21 days. The aliquots were then diluted, acidified and then subjected to ICP-OES for analysis of dissolved silicon. The result shown for dissolved Si (mg/L) in Figure 11 agrees well with the trend in pozzolanic behaviour: fly ash releasing the most silicon (most pozzolanic) and dacite releasing the least silicon (least pozzolanic).

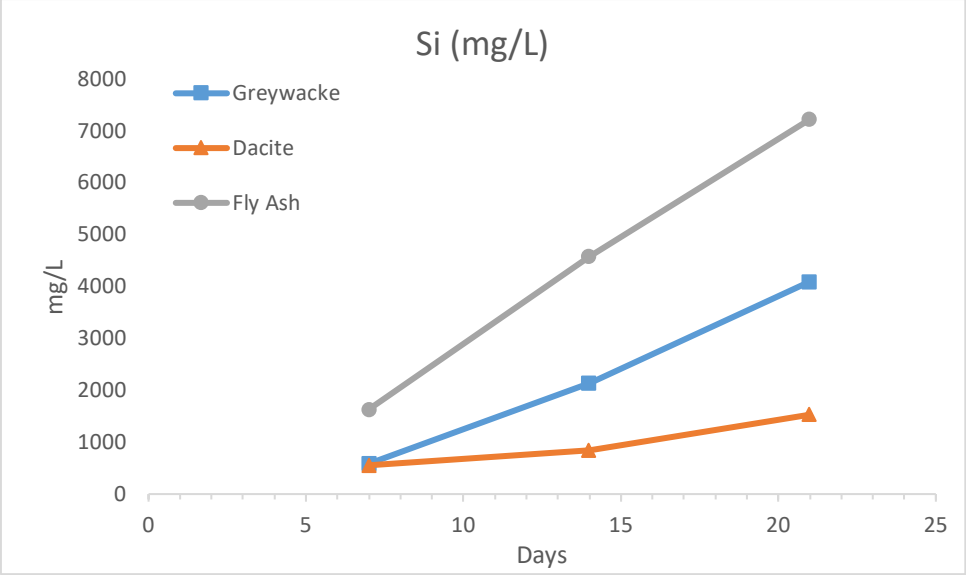

Figure 11 Dissolved silicon (Si) from the fly ash and reactive aggregate powders (dacite and greywacke) after 7, 14 and 21 days immersion in 1M NaOH at 80°C

Figure 12 shows the bar chart showing mass loss % corresponding to the hydrates (C-S-H and CH) quantified from the DTG curves. As can be observed, the different binder systems consume portlandite in similar order to the amount of C-S-H formed (i.e. OPC+FA25% consumed the most portlandite and therefore produced the most C-S-H, OPC has the most CH remaining and therefore produced the least C-S-H). The same trend can be observed at both 7 and 21 days (Figure 12a and b, respectively). Moreover, it is notable that whereas, C-S-H increases with time for all binder systems, CH only decreases when pozzolanic materials are present. For OPC, CH even minimally increased consistent with continued hydration reactions. There is not much difference in the amount of carbonates present (region within 600 to 800 °C in Figure 10). The quantified amount of carbonates ranged from 2.5-3%, which may just be due to the limestone content of Australian GP cements (maximum allowable limestone content is 7.5%).

Figure 13 shows the XRD of the pastes from 5 to 20 °2θ at 7 and 21 days. The intensity of the portlandite peak (P) of the different binder systems at 18° 2θ notably has the same order as the results from TG. OPC has the highest CH peak followed by OPC+FA25%, OPC+25%GW and OPC+25%DC. A decrease in the CH peak with time is also notable confirming the pozzolanicity of fly ash and the reactive aggregate powders. The absence of ettringite at

9.14 and 15.9 °2θ and monocarboaluminate peak at ~12 °2θ can also be observed consistent with their absence in the DTG curves in Figure 10.

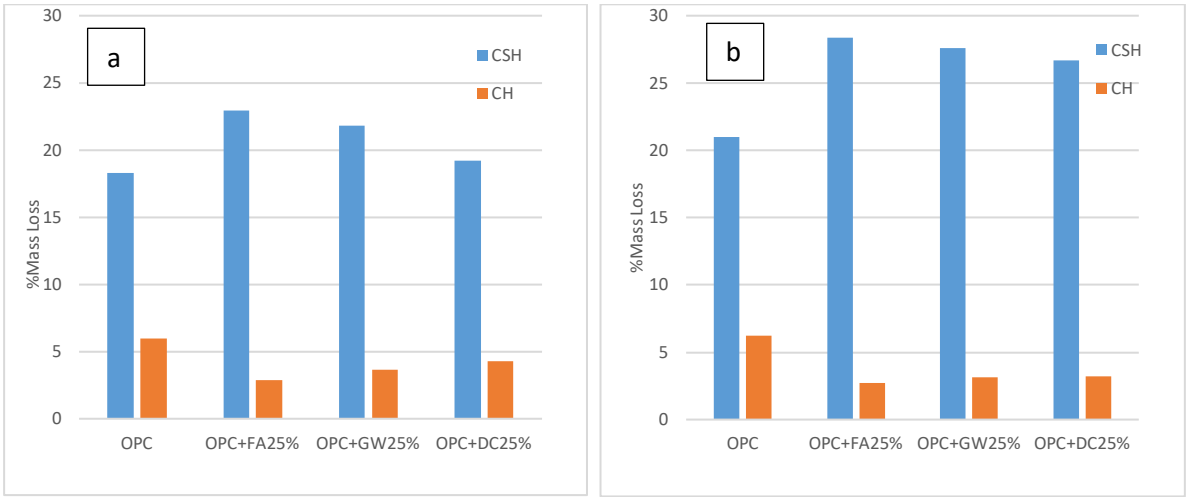

Figure 12 %Mass Loss for CH and CSH obtained from DTG curves at a) 7 days and b) 21 days

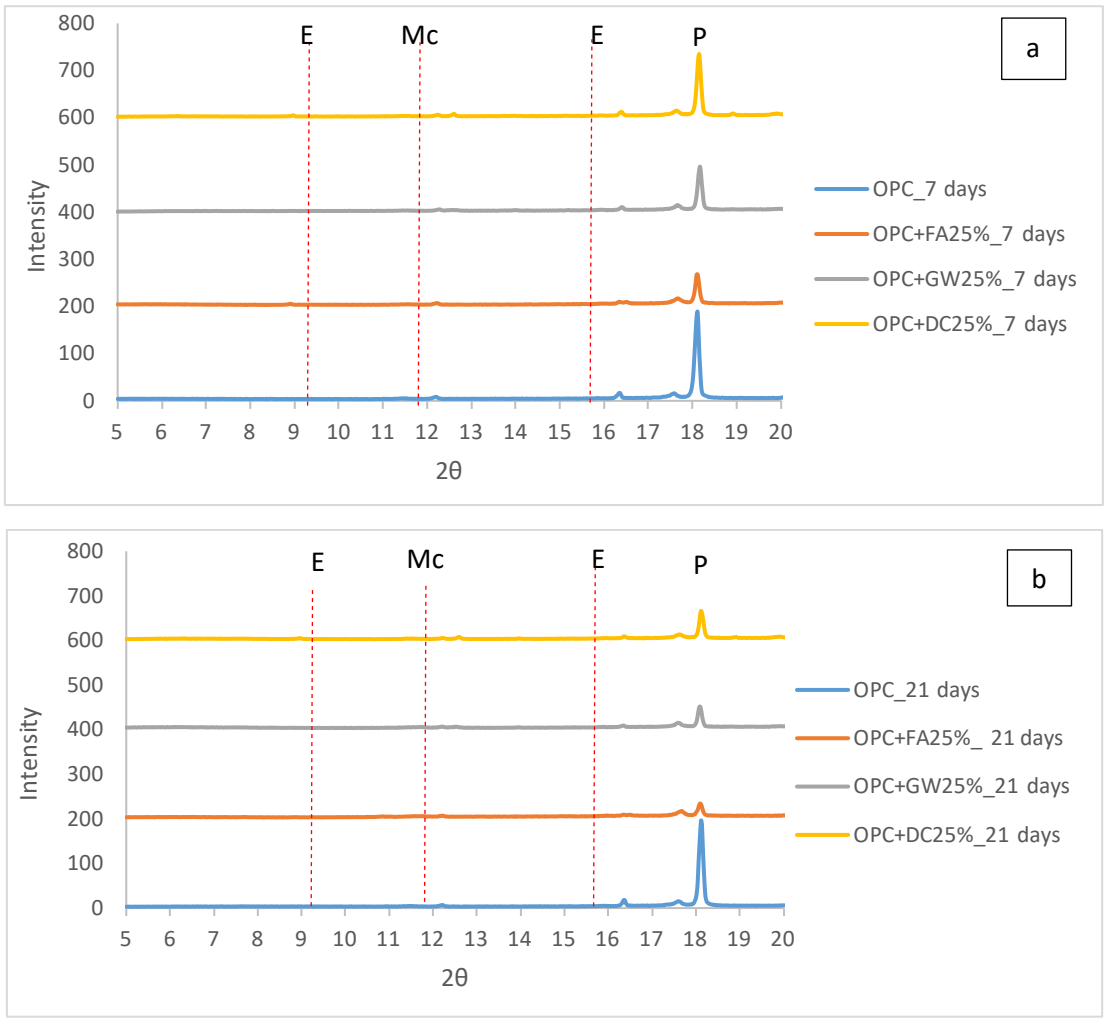

Figure 13 XRD of the pastes at a) 7 days and b) 21 days showing absence of ettringite (E) and carboaluminate (Mc) under AMBT conditions

3.4 Effect of the reactive aggregate powders on compressive strength

The compressive strength results in Figure 14 for mortars made with non-reactive sand show the effect of curing conditions on compressive strength development. Figure 14a clearly shows that AMBT accelerates early hydration resulting in significantly higher 7-day strength of mortars cured under AMBT conditions in comparison to those cured under normal hydration conditions. It is notable as well that at 7 days, the 25% fly ash mortar has the highest compressive strength, even higher than the plain OPC mortar. This indicates that AMBT increases the reactivity of fly ash consistent with what has been reported in literature [25]. High early strength can be correlated to a denser microstructure which can help reduce the rate of ingress of alkali from the AMBT bath. The high early age strength is attributed to increased rate of pozzolanic reactions due to higher temperature and alkalinity. Under normal curing conditions, SCMs also increase strength but this takes longer time because of much slower pozzolanic reactions [37].

In general, Figure 14b also shows the faster compressive strength development under AMBT conditions although it is notable that the OPC mortar (no SCM) has similar strength at 21 days regardless of the curing condition. This suggests that the AMBT conditions has accelerated the early age hydration of cement such that strength stabilization is reached early. The same can be said for the mortar+25% fly ash which did not exhibit much strength gain under AMBT conditions from 7 to 21 days. The mortar with 25% Dacite however has much lower compressive strength than OPC and fly ash regardless of curing condition. The decrease in strength with replacement of Dacite powder is however less than what would be expected from full dilution effect which suggests that the Dacite powder also contributes to microstructure densification although not as much as fly ash. This result is consistent with the TG results reported where fly ash is the most pozzolanic and formed highest amount of C-S-H, even higher than in the plain OPC paste.

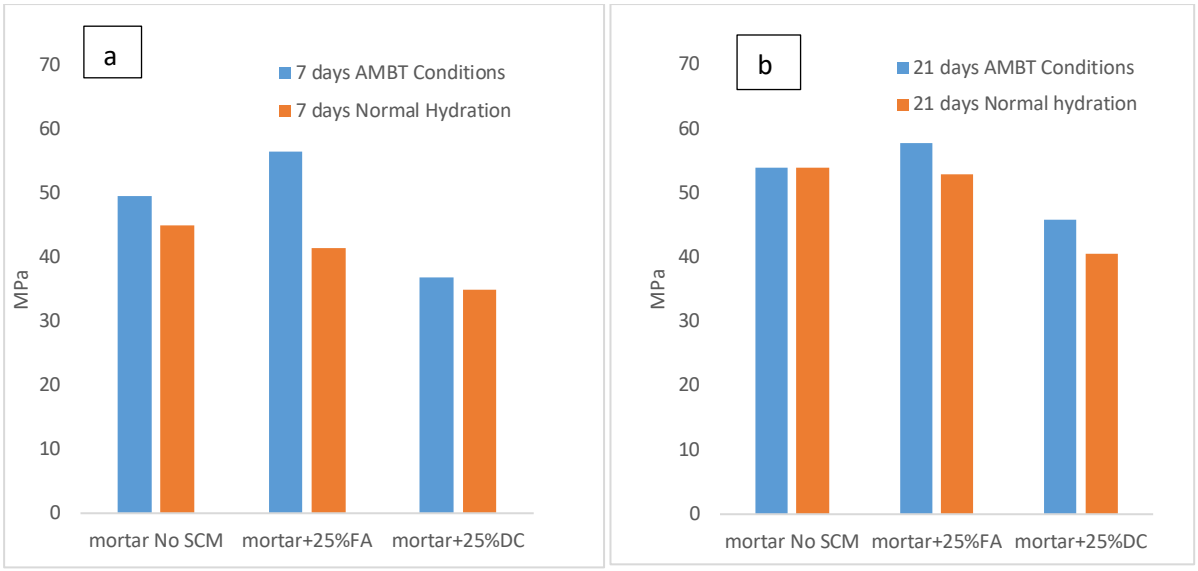

Figure 14 Effect of fly ash and reactive aggregate powder dacite on compressive strength of NR sand mortars at a) 7 days and b) 21 days AMBT and normal hydration conditions

The compressive strength results in Figures 15 and 16 for mortars made using the non-reactive sand and reactive Waikato sand respectively cured under AMBT conditions demonstrate similar trend at 7, 14 and 21 days. In general, in terms of compressive strength, mortar+25%fly ash > mortar no SCM > mortar+25%greywacke > mortar+25%dacite. Note that a higher w/c ratio was used for the Waikato mixes and thus a lower range of compressive strength than the non-reactive sand mortars is expected. The only notable difference from the two set of mixes is the slight drop in compressive strength over time in the mortars with reactive Waikato sand. The minimal drop in strength may be due to the microcracks observed in the SEM images due to ASR expansion. Greywacke powder however consistently showed much higher strength than dacite powder consistent with its ability to consume portlandite faster and form more C-S-H.

The difference in the effect of fly ash and the reactive aggregate powders on compressive strength development, is due not only to the difference in the "amorphous silica" content but may also be affected by the difference in particle size. Due to the slight difference in sizes of the powders and fly ash which is very notable from Figures 6-8, there is also an expected difference in the "filling effect" of the hydrates formed from pozzolanic reactions. It is possible that because fly ash is finer, the secondary C-S-H formed are able to better fill out the small voids in the binder better, therefore resulting in reduced porosity and increase in compressive strength. The effect of particle size was however not investigated in this study.

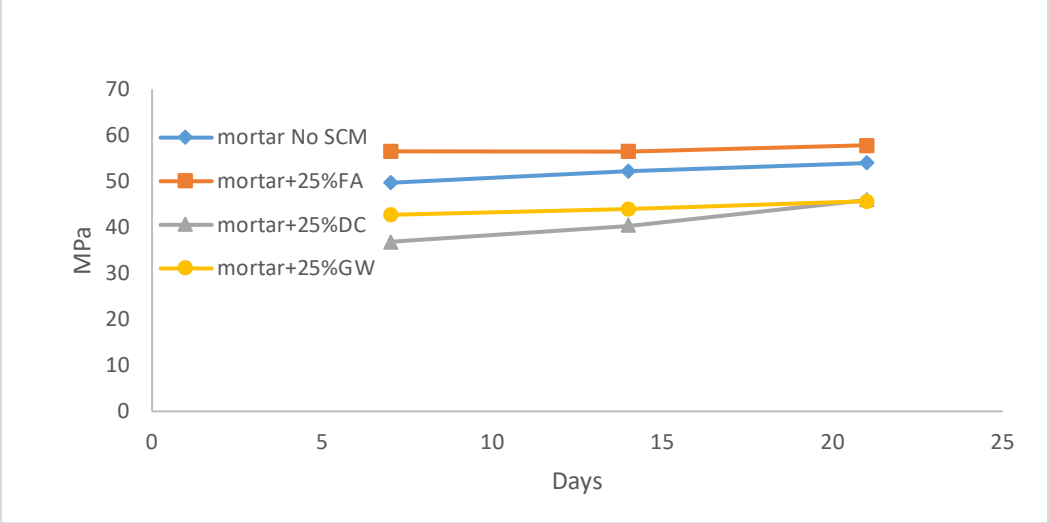

Figure 15 Effect of replacing cement with fly ash (FA), dacite powder (DC), greywacke powder (GW) in mortars with non-reactive sand under AMBT conditions

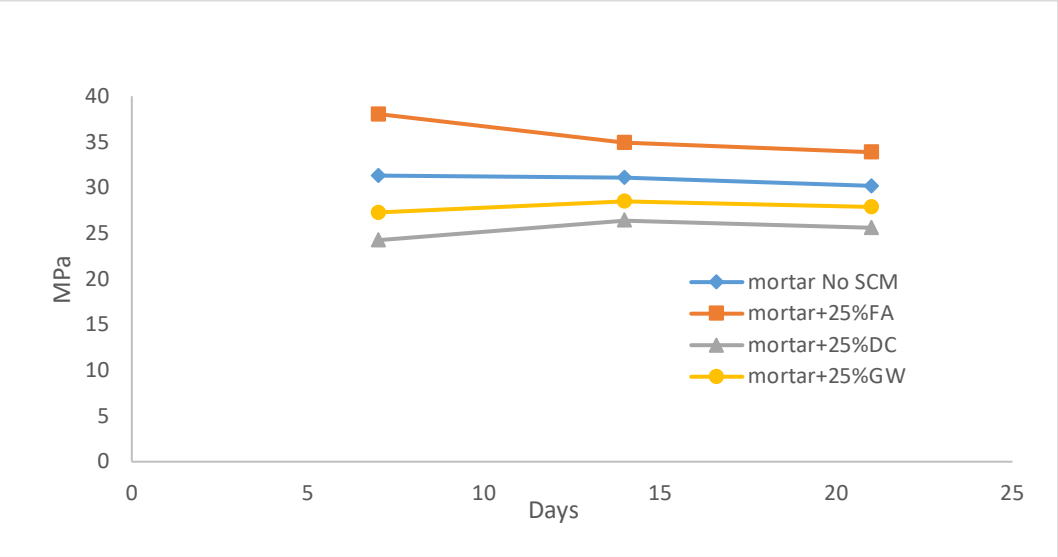

Figure 16 Effect of replacing cement with fly ash (FA), dacite powder (DC), greywacke powder (GW) in mortars with reactive sand Waikato under AMBT conditions

4.0 Conclusions

This study investigated the ability of reactive aggregate powders to mitigate ASR and compare the efficacy and mitigation mechanisms with that of fly ash. Below summarizes the important findings from this study.

1. Greywacke powder was able to reduce the ASR expansion to below 0.10% at 21 days while dacite powder was able to decrease expansion to below 0.30% at 21 days. These results are consistent with

488 the reduced amount of cracks observed in the sectioned mortars with reactive aggregate powders in
489 comparison to OPC mortar indicating their potential to be used as an alternate SCM for ASR mitigation.
490 Fly ash, however, is still better than the reactive aggregate powders in reducing ASR expansion when
491 used at a similar replacement level.
492
493 2. Thermogravimetric analysis shows that the reactive aggregate powders are pozzolanic like fly ash. Fly
494 ash is however notably more pozzolanic than both dacite and greywacke powder. The order of
495 pozzolanicity is as follows: OPC+25%fly ash>OPC+25%greywacke>OPC+25%dacite. Fly ash being the
496 most pozzolanic also formed the most amount of C-S-H. The order of pozzolanicity was found to be
497 consistent with their efficacy to mitigate ASR expansion.
498
499 3. Analysis of the C-S-H composition confirms that substituting cement with reactive aggregate powders
500 can lower the Ca/Si ratio and increase the Al/Si ratio. This modification in C-S-H composition is
501 consistent with the observed pozzolanic behaviour of the reactive aggregate powders and is reported
502 in literature to help enhance the alkali binding capacity of the C-S-H.
503
504 4. AMBT conditions accelerate compressive strength development of all mixes investigated. Replacing
505 cement with 25% fly ash also notably increases the compressive strength highlighting the contribution
506 of fly ash to microstructure densification. Although the reactive aggregate powders show a positive
507 effect on ASR mitigation, they do not help improve compressive strength. At all ages and regardless of
508 curing condition, the mortars with reactive aggregate powders exhibit lower compressive strength than
509 plain OPC mortar.
510
511 The study shows that reactive aggregate powders have the potential to mitigate ASR although higher dosages
512 ≥25% may be required to attain full ASR mitigating capability for a range of reactive aggregate powders. The
513 results also suggest that the primary mechanism by which reactive aggregate powders mitigate ASR is through
514 the consumption of portlandite (i.e. soluble calcium source) and modification of the C-S-H composition. The
515 observed negative effect of the reactive aggregate powders on compressive strength development may however
516 limit its potential application for mitigating ASR and therefore this area should be further investigated.

Moreover, as the particle size of the reactive aggregate powder is expected to affect compressive strength development as well as its efficacy in ASR mitigation, this factor is therefore also recommended to be investigated in future studies.

Acknowledgements

This study is a part of University of Technology Sydney research funded through Australian Research Council Research Hub for Nanoscience Based Construction Materials Manufacturing (NANOCOMM) with the support of Cement Concrete and Aggregates Australia (CCAA). This work would also not have been possible without laboratory equipment provided by Laboratory of Construction Materials at EPFL Switzerland courtesy of Professor Karen Scrivener.

References

1. Rajabipour, F., et al., *Alkali–silica reaction: Current understanding of the reaction mechanisms and the knowledge gaps.* Cement and Concrete Research, 2015. **76**: p. 130-146.
2. Thomas, M., *The effect of supplementary cementing materials on alkali-silica reaction: A review.* Cement and Concrete Research 2011. **41**: p. 1224–1231.
3. Standards Australia, *SA HB 79:2015 Alkali Aggregate Reaction—Guidelines on Minimising the Risk of Damage to Concrete Structures in Australia*. 2015, Standards Australia Limited.
4. Scrivener, K.L., V.M. John, and E.M. Gartner, *Eco-efficient cements: Potential economically viable solutions for a low-CO2 cement-based materials industry.* Cement and Concrete Research, 2018. **114**: p. 2-26.
5. Zerbino, R., et al., *Alkali–silica reaction in mortars and concretes incorporating natural rice husk ash.* Construction and Building Materials, 2012. **36**: p. 796–806.
6. Abbas, S., S.M.S. Kazmi, and M.J. Munir, *Potential of rice husk ash for mitigating the alkali-silica reaction in mortar bars incorporating reactive aggregates.* Construction and Building Materials 2017. **132**: p. 61–70.
7. Kazmia, S.M.S., et al., *Pozzolanic reaction of sugarcane bagasse ash and its role in controlling alkali silica reaction.* Construction and Building Materials 2017. **148**: p. 231–240.
8. Shi, C., et al., *Characteristics and Pozzolanic Reactivity of Glass Powders.* Cement and Cocrete Research, 2005. **35**: p. 987-993.
9. Omrana, A.F., et al., *Long-term performance of glass-powder concrete in large-scale field applications.* Construction and Building Materials 2017. **135**: p. 43–58.
10. Zheng, K., *Pozzolanic reaction of glass powder and its role in controlling alkali silica reaction.* Cement and Concrete Composites 2016. **67**: p. 30-38.
11. Thomas, B.S., et al., *Biomass ashes from agricultural wastes as supplementary cementitious materials or aggregate replacement in cement/geopolymer concrete: A comprehensive review.* Journal of Building Engineering, 2021. **40**: p. 102332.
12. Esteves, T.C., et al., *Use of biomass fly ash for mitigation of alkali-silica reaction of cement mortars.* Construction and Building Materials, 2012. **26**(1): p. 687-693.
13. Afshinnia, K. and P.R. Rangaraju, *Influence of fineness of ground recycled glass on mitigation of alkali–silica reaction in mortars.* Construction and Building Materials, 2015. **81**: p. 257-267.

14. Afshinnia, K. and A. Poursaee, *The potential of ground clay brick to mitigate Alkali–Silica Reaction in mortar prepared with highly reactive aggregate.* Construction and Building Materials, 2015. **95**: p. 164-170.
15. Bektas, F. and K. Wang, *Performance of ground clay brick in ASR-affected concrete: Effects on expansion, mechanical properties and ASR gel chemistry.* Cement & Concrete Composites 2012. **34**: p. 273–278.
16. Cyr, M., P. Rivard, and F. Labrecque, *Reduction of ASR-expansion using powders ground from various sources of reactive aggregates.* Cement & Concrete Composites, 2009. **31**: p. 438–446.
17. Standards Australia, *AS 1141.60.1 Methods for sampling and testing aggregates Method 60.1: Potential Alkali-Silica Reactivity-Accelerated Mortar Bar Method*. 2014, Standards Australia Limited: Sydney, Australia.
18. Sirivivatnanon, V., J. Mohammadi, and W. South, *Reliability of new Australian test methods in predicting alkali silica reaction of field concrete.* Construction and Building Materials, 2016. **126**: p. 868-874.
19. Sirivivatnanon, V., et al., *Reliability of extending AS1141.60.1 and 60.2 test methods to determine ASR mitigation*, in *Concrete 2019: Concrete in Practice-Progress Through Knowledge*. 2019, Concrete Institute of Australia: Sydney, Australia.
20. Munir, M.J., et al., *Role of test method in detection of alkali–silica reactivity of concrete aggregates.* Proceedings of the Institution of Civil Engineers - Construction Materials, 2018. **171**(5): p. 203-221.
21. Standards Australia, *AS 3972 General Purpose and Blended Cements*. 2010: Sydney, Australia.
22. Standards Australia, *AS 3582.1: Supplementary cementitious materials - Fly ash*. 2016: Sydney, Australia.
23. ASTM International, *ASTM C1567 Standard Test Method for Determining the Potential Alkali-Silica Reactivity of Combinations of Cementitious Materials and Aggregate (Accelerated Mortar-Bar Method)*. 2013: West Conshohocken, Pennsylvania, United States.
24. Rossen, J.E. and K.L. Scrivener, *Optimization of SEM-EDS to determine the C–A–S–H composition in matured cement paste samples.* Materials Characterization, 2017. **123**: p. 294-306.
25. Shafaatian, S.M.H., et al., *How does fly ash mitigate alkali–silica reaction (ASR) in accelerated mortar bar test (ASTM C1567)?* Cement & Concrete Composites 2013. **37**: p. 143–153.
26. Tapas, M.J., et al., *Influence of Limestone Mineral Addition in Cements on the Efficacy of SCMs in Mitigating Alkali-Silica Reaction Assessed by Accelerated Mortar Bar Test.* Journal of Materials in Civil Engineering, 2021.
27. Leemann, A., *Raman microscopy of alkali-silica reaction (ASR) products formed in concrete.* Cement and Concrete Research, 2017. **102**: p. 41-47.
28. Leemann, A., et al., *Types of alkali–aggregate reactions and the products formed.* Proceedings of the Institution of Civil Engineers. Construction materials, 2016. **169**(3): p. 128-135.
29. Tapas, M.J., et al., *Efficacy of SCMs to mitigate ASR in systems with higher alkali contents assessed by pore solution method.* Cement and Concrete Research, 2021. **142**: p. 106353.
30. Thaulow, N., U.H. Jakobsen, and B. Clark, *Composition of alkali silica gel and ettringite in concrete railroad ties: SEM-EDX and X-ray diffraction analyses.* Cement and concrete research, 1996. **26**(2): p. 309-318.
31. Hong, S.-Y. and F.P. Glasser, *Alkali sorption by C-S-H and C-A-S-H gels Part II. Role of alumina.* Cement and Concrete Research, 2002. **32**: p. 1101–1111.
32. Lothenbach, B., K. Scrivener, and R.D. Hooton, *Supplementary cementitious materials.* Cement and Concrete Research 2011. **41**: p. 1244–1256.
33. Lothenbach, B., P. Durdziński, and K.D. Weerdt, *Thermogravimetric analysis*, in *A Practical Guide to Microstructural Analysis of Cementitious Materials*, K. Scrivener, R. Snellings, and B. Lothenbach, Editors. 2016, Taylor and Francis.
34. Taylor, H., C. Famy, and K. Scrivener, *Delayed Ettringite Formation.* Cement and Concrete Research, 2001. **31**: p. 683-693.
35. Matschei, T., B. Lothenbach, and F.P. Glasser, *Thermodynamic properties of Portland cement hydrates in the system $CaO–Al_2O_3–SiO_2–CaSO_4–CaCO_3–H_2O$.* Cement and Concrete Research 2007. **37**: p. 1379–1410.
36. Wang, H. and J.E. Gillott, *Mechanism of alkali-silica reaction and the significance of calcium hydroxide.* Cement and Concrete Research, 1991. **21**(4): p. 647-654.
37. Juenger, M.C.G. and R. Siddique, *Recent advances in understanding the role of supplementary cementitious materials in concrete.* Cement and Concrete Research 2015. **78**: p. 71–80.